	a_u			b_u		
	2	3	4	2	3	4
Exptl	0.3	0.7	1.0	0.5	0.3	0.6_5
Calcd	0.21	0.57	1.0	0.57	0.39	0.75

a_g		
2	3	4
0.6	0.4	0.8_5
0.57	0.39	0.75

(41) M. Rohmer, J. Demuynek, and A. Veilland, *Theor. Chim. Acta*, **36**, 93–102 (1974).
(42) I. Hillier, M. Guest, R. Higginson, and D. Lloyd, *Mol. Phys.*, **27**, 215 (1974).
(43) B. Mann, R. Pietropaolo, and B. Shaw, *J. Chem. Soc., Dalton Trans.*, 2390 (1973).
(44) Koopmans, of course, did not intend to apply this relationship to open shell cases, but with modifications they can be considered; cf. P. A. Cox et al., *Struct. Bonding (Berlin)*, **24**, 59 (1975).
(45) E. Heilbronner, Organic Photoelectron Spectroscopy, Sixth Conference on Molecular Spectroscopy, Durham, *in* press.

The Mechanism of Ligand Dissociation in Group 8 ML_5 Complexes

A. D. English,* P. Meakin,* and J. P. Jesson*

Contribution No. 2250 from the Central Research and Development Department, Experimental Station, E. I. du Pont de Nemours and Company, Wilmington, Delaware 19898. *Received February 25, 1976*

Abstract: Free energies of activation ($\Delta G^{\ddagger}$) for dissociation in the equilibrium $M[P(OC_2H_5)_3]_5^{n+} \rightleftharpoons M[P(OC_2H_5)_4]_4^{n+} + P(OC_2H_5)_3$ have been determined for M = Co(I), Rh(I), Ir(I), Ni(II), Pd(II), Pt(II), together with $\Delta G^{\ddagger}$ values for dissociation in the equilibrium $RhL_5^+ \rightleftharpoons RhL_4^+ + L$ with L = $P(OCH_3)_3$, $P(OC_2H_5)_3$, $P(O\text{-}n\text{-}C_3H_7)_3$, $P(O\text{-}n\text{-}C_4H_9)_3$, and $P(OCH_2)_3CCH_3$. The relationship between these parameters and the corresponding $\Delta G^{\ddagger}$ values for intramolecular exchange in the ML_5 compounds is discussed and evidence is presented to suggest a similarity between the reaction coordinates for intramolecular rearrangement and ligand dissociation. In particular, the planar association–trigonal bipyramidal reaction coordinate appears to involve tetragonal pyramidal intermediates or transition states, implying that the axial ligands in the trigonal bipyramid do not remain collinear with the metal throughout the reaction, as has been assumed in the current picture for planar substitution. For M = Rh and L = *n*-alkyl phosphite, it is suggested that two competing steric effects—crowding in the tetragonal pyramid and the steric assist to bond breaking—offset one another to give a free energy of activation for dissociation nearly independent of the steric size of L. The data were obtained from a line shape analysis of $^{31}P\{^1H\}$ NMR spectra as a function of temperature. The calculations employed are described in detail, using two-, three-, four- and five-site one-spin models, to show the origin of *unexpected line width increases* in the RhL_5^+ $^{31}P\{^1H\}$ doublet, at temperatures above the slow exchange limit as the [Rh]/[L] ratio is either *increased* or *decreased* from the value 1/5, assuming a first-order dissociation process. In some instances, equilibrium constants have been measured for the ligand dissociation reaction using spectrophotometric techniques.

Recent low temperature NMR studies[1-5] have shown that a wide range of group 8 ML_5 complexes have trigonal bipyramidal (D_{3h}) geometries in solution. At higher temperatures, both intramolecular and intermolecular exchange processes take place at rates which make NMR line shape investigations possible. In most cases, the free energies of activation are considerably higher for intermolecular exchange so that the two processes can be treated separately. Detailed line shape analyses[3,5] show that the intramolecular rearrangement mechanism involves simultaneous exchange of the two axial ligands with two equatorial ligands. A systematic investigation of the variation of the barriers to intramolecular rearrangement with the nature of the phosphorus ligand and the nature of the central metal has been reported[5] and preliminary $^{31}P\{^1H\}$ NMR studies of *intermolecular* exchange behavior[3,4] in $Rh[P(OCH_3)_3]_5^+$ have established a first-order dissociative mechanism.

In the present paper, we describe the details of a systematic $^{31}P\{^1H\}$ study of the *intermolecular* exchange behavior in these complexes, varying the ligand and the central metal. The data are all consistent with a simple dissociative process (eq 1); the free energies of activation for dissociation correlate closely with previously established free energies of activation for intramolecular rearrangement[5] suggesting similar square pyramidal transition states for two processes.

$$ML_5^{n+} \underset{k_{-1}}{\overset{k_1}{\rightleftharpoons}} ML_4^{n+} + L \qquad (1)$$

Our recent predictions[4] for the dependence of the line widths in the RhL_5^+ doublet on [L]/[Rh] in the $RhL_5^+/RhL_4^+/L$ system near the slow exchange limit have been confirmed both experimentally and theoretically using the five-site model. Line shape calculations are described which clearly indicate why dramatic line width increases in the $^{31}P\{^1H\}$ doublet of RhL_5^+ occur at certain temperatures, when the metal to ligand ratio is either increased or decreased from 1/5, assuming a simple dissociative process. Similar line shape effects are calculated for $ML_5^{n+}/ML_4^{n+}/L$ systems in which the central metal M has no nuclear spin.

Previous two-, three-, and four-site models used to calculate the $^{31}P\{^1H\}$ NMR line shapes for "ML_5^+" ([ML_5^+] → 0, [L] → 0), "ML_5^+/L" ([ML_4^+] → 0), and "ML_5^+/ML_4^+" ([L] → 0), for the case where M = Rh, are justified both numerically and analytically.

Experimental Section

Methods of preparation of the complexes have been described earlier[2] as have the general nuclear resonance techniques employed.[1-3] In cases where small variations in rate from one system to another were important (e.g., effect of change of solvent on reaction rate), relative orderings were established by sequential measurements at a single temperature, instead of (or in addition to) complete temperature variation studies on each system separately. Spectrophotometric studies were carried out using a Cary 41 spectrophotometer.

Intermolecular Exchange Calculations. Data were presented earlier[4] for intermolecular exchange behavior in $Rh[P(OCH_3)_3]_5^+/$

$Rh[P(OCH_3)_3]_4^+/L$ systems. The results were interpreted on the basis of a simple dissociative process (eq 1); the interpretation revealed a number of unusual features in the line shape behavior which might appear to be inconsistent with a dissociative mechanism. It has become apparent that the description in ref 4 does not show clearly how these apparent inconsistencies arise. The points are crucial in establishing mechanistic information for ligand exchange processes from NMR line shape studies. We have therefore included the following sections in the present paper to try to clarify the situation.

(a) The Elimination of Sites of Very Low Concentration in NMR Line Shape Calculations. If the populations of one or more sites in a multisite exchange problem are very low, and if the preexchange lifetimes of these sites are very short compared to the reciprocal of the frequency separations from other sites, the time development of the spin density matrices at these sites can be ignored.[6] The effect of the low population sites reduces to that of additional exchange terms (reaction paths) between the more populated sites. Consequently, sites of very low population can be eliminated from the NMR line shape calculations if the exchange terms between the other sites are suitably modified. The elimination of low population sites has two beneficial effects: (a) The dimension of the complex non-Hermitian matrix, which must be diagonalized[7-9] in order to calculate the NMR line shapes, is reduced. (b) The dynamic range of the elements in the exchange matrix is reduced, resulting in an improvement in the numerical stability of the line shape calculations.

We have previously used this method for simplifying NMR line shape analysis in systems undergoing intermolecular exchange.[4,10] Its application to the reduction of the five-site model for the $RhL_5^+/RhL_4^+/L$ system (shown in Figure 1) to the two-, three-, and four-site models used in our earlier work[4] is discussed below.

Ignoring the effects of relaxation, the "density matrix" equations of motion for the five-site one-spin (^{31}P) model shown in Figure 1 are[11]

$$\frac{d\rho_1}{dt} = -i\mathcal{L}_1\rho_1 - k_1\rho_1 + k_1\frac{[ML_5^+]}{[ML_4^+]}\rho_3 + k_1\frac{[ML_5^+]}{2[L]}\rho_5 \quad (2A)$$

$$\frac{d\rho_2}{dt} = -i\mathcal{L}_2\rho_2 - k_1\rho_2 + k_1\frac{[ML_5^+]}{[ML_4^+]}\rho_4 + k_1\frac{[ML_5^+]}{2[L]}\rho_5 \quad (2B)$$

$$\frac{d\rho_3}{dt} = -i\mathcal{L}_3\rho_3 - k_1\frac{[ML_5^+]}{[ML_4^+]}\rho_3 + \frac{4k_1}{5}\rho_1 \quad (2C)$$

$$\frac{d\rho_4}{dt} = -i\mathcal{L}_4\rho_4 - k_1\frac{[ML_5^+]}{[ML_4^+]}\rho_4 + \frac{4k_1}{5}\rho_2 \quad (2D)$$

$$\frac{d\rho_5}{dt} = -i\mathcal{L}_5\rho_5 - k_1\frac{[ML_5^+]}{[L]}\rho_5 + \frac{k_1}{5}(\rho_1 + \rho_2) \quad (2E)$$

where $\mathcal{L}_i$ is the Liouville operator for the ith site, and k_1 is the forward rate constant for the reaction given in eq 1. In order to calculate NMR line shapes, eq 2 is solved in a coordinate system rotating at the frequency of the applied rf field and the symbols ρ_i and $\mathcal{L}_i$ should be replaced by $\rho_i{}^\omega$ and $\mathcal{L}_i{}^\omega$. The absorption intensity at frequency ω is given by

$$I(\omega) \propto I_m(\rho^\omega \cdot \mathbf{M}^-) \quad (3)$$

where ρ^ω is the density vector in composite Liouville space[12] [$\rho^\omega = (\rho_1{}^\omega, \rho_2{}^\omega, \ldots, \rho_n{}^\omega)$, n is the number of sites] and $\mathbf{M}^-$ is a vector in composite Liouville space containing the vectors $\mathbf{M}_i{}^-$. $\mathbf{M}_i{}^-$ contains the elements of the operator $\mathbf{M}_i{}^- = \gamma_{ij}I_{ij}{}^-$ where $I_{ij}{}^-$ is the spin lowering operator in ordinary Hilbert space for the jth spin at the ith site; γ_{ij} is the corresponding magnetogyric ratio. Only the elements of ρ^ω corresponding to the nonzero elements of $\mathbf{M}^-$ are needed to calculate $I(\omega)$ using eq 2. Assuming the conditions of slow passage, high temperature, and weak radio frequency fields, eq 2 gives the expressions

$$-i\mathcal{L}_1\rho_1 - k_1\rho_1 + k_1\frac{[ML_5^+]}{[ML_4^+]}\rho_3 + k_1\frac{[ML_5^+]}{2[L]}\rho_5 = P_1\mathbf{M}_1{}^- \quad (4A)$$

$$-i\mathcal{L}_2\rho_2 - k_1\rho_2 + k_1\frac{[ML_5^+]}{[ML_4^+]}\rho_4 + k_1\frac{[ML_5^+]}{2[L]}\rho_5 = P_2\mathbf{M}_2{}^- \quad (4B)$$

$$-i\mathcal{L}_3\rho_3 - k_1\frac{[ML_5^+]}{[ML_4^+]}\rho_3 + \frac{4k_1}{5}\rho_1 = P_3\mathbf{M}_3{}^- \quad (4C)$$

$$-i\mathcal{L}_4\rho_3 - k_1\frac{[ML_5^+]}{[ML_4^+]}\rho_4 + \frac{4k_1}{5}\rho_2 = P_4\mathbf{M}_4{}^- \quad (4D)$$

$$i\mathcal{L}_5\rho_5 - k_1\frac{[ML_5^+]}{[L]}\rho_5 + \frac{k_1}{5}(\rho_1 + \rho_2) = P_5\mathbf{M}_5{}^- \quad (4E)$$

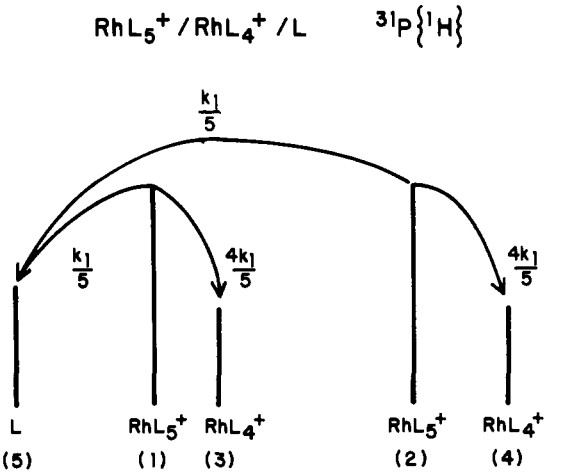

Figure 1. Exchange diagram for five-site (one spin) model used to calculate intermolecular exchange behavior for $RhL_5^+/RhL_4^+/L$ solutions. Only the forward reaction path is shown in the diagram. The reverse paths must, of course, be included in setting up the exchange matrix.

for the density matrix elements one off diagonal in I_z needed to calculate $I(\omega)$ using eq 3. The coefficients P_i in eq 4 are proportional to the site populations. The steady state assumption, $(d\rho/dt = 0)$, which is justified by the slow passage conditions; was used to obtain eq 4A-E. The symbols ρ_i and $\mathcal{L}_i$ are used in place of $(\rho_i{}^\omega)_{od}$ and $(\mathcal{L}_i{}^\omega)_{od}$ in eq 4A-E and subsequent equations for the sake of notational simplicity. The subscript od indicates that only elements whose indices are one off diagonal in I_z are induced.

If the concentration of free ligand L is very small and k_1 is sufficiently large, such that the preexchange lifetime of the free ligand is short compared to the inverse frequency separation for the five sites we have

$$k_1\frac{[ML_5^+]}{[L]}\mathbf{E} \gg i(\mathcal{L}_5{}^\omega)_{od} \quad (5)$$

where $\mathbf{E}$ is the unit matrix for frequencies in the region over which the NMR line shapes are calculated.[13] Using the relationship given in eq 5, in eq 4E we obtain the approximate result

$$\frac{[ML_5^+]}{[L]}\rho_5 \approx \frac{1}{5}(\rho_1 + \rho_2) - \frac{1}{k_1}P_5\mathbf{M}_5{}^- \quad (6)$$

This approximate relationship allows us to eliminate ρ_5 from eq 4A and 4B giving the expressions

$$-i\mathcal{L}_1\rho_1 - \frac{9k_1}{10}\rho_1 + k_1\frac{[ML_5^+]}{[ML_4^+]}\rho_3 + \frac{k_1}{10}\rho_2 \approx P_1\mathbf{M}_1{}^- + (P_5/2)\mathbf{M}_5{}^- \quad (7A)$$

$$-i\mathcal{L}_2\rho_2 - \frac{9k_1}{10}\rho_2 + k_1\frac{[ML_5^+]}{[ML_4^+]}\rho_4 + \frac{k_1}{10}\rho_1 \approx P_2\mathbf{M}_2{}^- + (P_5/2)\mathbf{M}_5{}^- \quad (7B)$$

and since $P_5 \ll P_1$, $P_5 \ll P_2$

$$-i\mathcal{L}_1\rho_1 - \frac{9k_1}{10}\rho_1 + k_1\frac{[ML_5^+]}{[ML_4^+]}\rho_3 + \frac{k_1}{10}\rho_2 \approx P_1\mathbf{M}_1{}^- \quad (8A)$$

$$-i\mathcal{L}_2\rho_2 - \frac{9k_1}{10}\rho_2 + k_1\frac{[ML_5^+]}{[ML_4^+]}\rho_4 + \frac{k_1}{10}\rho_1 \approx P_2\mathbf{M}_2{}^- \quad (8B)$$

(8C) = (4C), (8D) = (4D)

Equations 8A-D can be obtained directly from the four-site model introduced earlier[4] for calculating NMR line shapes in the RhL_5^+/RhL_4^+ system.

Similarly, if the ML_4^+ cation is present in only very low concentrations, eq 4C and 4D give

$$\frac{[ML_5^+]}{[ML_4^+]}\rho_3 \approx {}^4/_5\rho_1 - \frac{1}{k_1}P_3\mathbf{M}_3{}^- \quad (9A)$$

$$\frac{[ML_5^+]}{[ML_4^+]}\rho_4 \approx {}^4/_5\rho_2 - \frac{1}{k_1}P_4\mathbf{M}_4{}^- \quad (9B)$$

Using these results and inequalities $P_3 \ll P_1$, $P_4 \ll P_2$ to eliminate ρ_3 and ρ_4 from eq 4A and 4B, the results

$$-i\mathcal{L}_1\rho_1 - \frac{k_1}{5}\rho_1 + k_1\frac{[ML_5^+]}{2[L]}\rho_5 \approx P_1\mathbf{M}_1^- \quad (10A)$$

$$-i\mathcal{L}_2\rho_2 - \frac{k_1}{5}\rho_2 + k_1\frac{[ML_5^+]}{2[L]}\rho_5 \approx P_2\mathbf{M}_2^- \quad (10B)$$

and (10C) = (4E) are obtained. Equations 10A, 10B, and 10C can be derived from the three-site model[4] used to analyze NMR line shapes for the ML_5^+/L system. Finally, the two-site model used to calculate NMR line shapes for ML_5^+ solutions, in which the degree of dissociation is small, can be obtained directly from eq 2A–E assuming $[L] \rightarrow 0$ and $[ML_4^+] \rightarrow 0$ or from the three-site or four-site models.

The procedure outlined above for simplifying the NMR line shape calculation for the $RhL_5^+/RhL_4^+/L$ system can be applied in a wide variety of circumstances. If ρ_A is a density vector in composite Liouville space containing the density matrix elements of the major species and ρ_B is a similar density vector containing the density matrix elements for the low concentration species, the density matrix equation of motion can be written as

$$\frac{d\rho_A}{dt} = -i\mathcal{L}_A\rho_A + \chi_{AA}\rho_A + \chi_{AB}\rho_B \quad (11A)$$

$$\frac{d\rho_B}{dt} = -i\mathcal{L}_B\rho_B + \chi_{BA}\rho_A + \chi_{BB}\rho_B \quad (11B)$$

where the χ's are exchange matrices in Liouville space.

The density matrix elements one off diagonal in I_z can then be calculated from the expression

$$-i\mathcal{L}_A{}^{\omega}(\rho_A{}^{\omega})_{od} + \chi_{AA}(\rho_A{}^{\omega})_{od} + \chi_{AB}(\rho_B{}^{\omega})_{od} = \sigma_A \quad (12A)$$

$$-i\mathcal{L}_B{}^{\omega}(\rho_B{}^{\omega})_{od} + \chi_{BA}(\rho_A{}^{\omega})_{od} + \chi_{BB}(\rho_B{}^{\omega})_{od} = \sigma_B \quad (12B)$$

In the above equations, σ_A and σ_B are vectors containing the elements of the $\mathbf{M}_i^-$ operators for the major and minor species, respectively, weighted by the appropriate populations. Using the inequality[13] $i\mathcal{L}_B \ll \chi_{BB}$ and noting that the elements of σ_B are much smaller than those of σ_A, eq 12B can be used to eliminate $(\rho_B{}^{\omega})_{od}$ from eq 12A giving the result

$$-i\mathcal{L}_A{}^{\omega}(\rho_A{}^{\omega})_{od} + \chi_{AA}(\rho_A{}^{\omega})_{od} - \chi_{AB}\chi_{BB}{}^{-1}\chi_{BA}(\rho_A{}^{\omega})_{od} \approx \sigma_A \quad (13)$$

which can be used to calculate the NMR line shapes. Equation 13 can be obtained from the equation of motion (eq 14.) The last term in this equation describes the kinetic effects of the low concentration species.

$$\frac{d\rho_A}{dt} \approx -i\mathcal{L}_A\rho_A + \chi_{AA}\rho_A - \chi_{AB}\chi_{BB}{}^{-1}\chi_{BA}\rho_A \quad (14)$$

Since the dimensions of the matrices which must be manipulated to solve eq 13 are smaller than that required to solve eq 12 and since the computer time required to invert a large matrix or to multiply matrices is much less than that required to diagonalize a complex non-Hermetian matrix of the same dimension, considerable savings in computer time can be realized. In many cases, it is preferable to eliminate sites of low population by means of analytic rather than numerical methods.

(b) The Five-Site Model for the Case Where the Central Metal Has a Spin of ½. In our earlier work,[4] line shape analyses were carried out for the $RhL_5^+/RhL_4^+/L$ system using two- (RhL_5^+), three- (RhL_5^+/L), and four-(RhL_5^+/RhL_4^+) site models which may be obtained from the five-site model (Figure 1) by eliminating sites of low population (vide supra). It was observed that addition of ligand (at constant temperature) to solutions of RhL_5^+, at temperatures below coalescence but above the slow exchange limit, increased the width of the "RhL_5^+" resonances in the $^{31}P\{^1H\}$ spectrum. A similar but more pronounced broadening is observed on adding RhL_4^+. A superficial interpretation of these results would lead to the conclusion that the broadening of the RhL_5^+ resonances by addition of either L or RhL_4^+ is a result of acceleration of the intermolecular exchange by both L and RhL_4^+ and that the results are inconsistent with the process

$$RhL_5^+ \underset{k_{-1}}{\overset{k_1}{\rightleftharpoons}} RhL_4^+ + L \quad (15)$$

being the sole exchange mechanism. In this section, the five-site model shown in Figure 1 is used to demonstrate that the proposed mechanism (eq 15) can be used to predict all of the general features of the experimental observations.

Equations 2 and 3 lead to the line shape expression (eq 16) for the five-site model where $I(\omega)$ is the intensity at angular frequency ω, the ω_i are the angular frequencies for the five sites, and T_2 is the transerse relaxation time assumed to be equal at all five sites. Equation 16 may be written in a more compact form as eq 17

$$I(\omega) = -Re\{\mathbf{P}\cdot[\chi + \mathbf{R} - i\mathcal{L}_0(\omega)]^{-1}\cdot\mathbf{1}\} \quad (17)$$

where $\mathbf{P}$ is a vector containing the site populations, χ is a matrix describing the exchange process, and $\mathbf{R}$ is the relaxation matrix. The vector $\mathbf{1}$ is the unit vector (1 1 1 1 1) which represents $\mathbf{M}^-$ in this case.

We are assuming, as confirmed by the data, that all ligands of a given RhL_5^+ or RhL_4^+ are equivalent due to chemical exchange or intrinsic magnetic equivalence. (These considerations are implicit in the previous section and in the discussion which follows.)

The diagonal elements of χ represent the rates at which species leave the different sites; thus, for the two ML_5^+ sites (1 and 2)

$$d[ML_5^+]/dt = -k_1[ML_5^+] \quad (18)$$

so that $\chi_{11} = \chi_{22} = -k_1$. Similarly, for the two ML_4^+ sites,

$$\frac{d[ML_4{}^1]}{dt} = -k_{-1}[L][ML_4^+] = \left\{-\frac{k_1[ML_5^+]}{[ML_4{}^1]}\right\}[ML_4^+] \quad (19)$$

with the pseudo-first order-rate constant $(k_1[ML_5^+]/[ML_4^+])$ thus,

$$\chi_{33} = \chi_{44} = -k_1[ML_5^+]/[ML_4^+]$$

$$I(\omega) = -Re\{[5[ML_5^+]/2,\ 5[ML_5^+]/2,\ 4[ML_4^+]/2,\ 4[ML_4^+]/2,\ [L]]$$

$$\begin{bmatrix} -k_1 - (1/T_2) + i(\omega_1 - \omega) & 0 & 4k_1/5 & 0 & k_1/5 \\ 0 & -k_1 - (1/T_2) + i(\omega_2 - \omega) & 0 & 4k_1/5 & k_1/5 \\ k_1[ML_5^+]/[ML_4^+] & 0 & (-k_1[ML_5^+]/[ML_4^+]) - (1/T_2) + i(\omega_3 - \omega) & 0 & 0 \\ 0 & k_1[ML_5^+]/[ML_4^+] & 0 & (-k_1[ML_5^+]/[ML_4^+]) - (1/T_2) + i(\omega_4 - \omega) & 0 \\ (k_1/2) \times ([ML_5^+]/[L]) & (k_1/2) \times ([ML_5^+]/[L]) & 0 & 0 & -k[ML_5^+]/[L] - (1/T_2) + i(\omega_5 - \omega) \end{bmatrix}^{-1} \begin{bmatrix} 1 \\ 1 \\ 1 \\ 1 \\ 1 \end{bmatrix} \quad (16)$$

Finally, for the L site

$$\frac{d[L]}{dt} = -k_{-1}[ML_4^+][L] = -\left\{k_1\frac{[ML_5^+]}{L}\right\}[L] \qquad (20)$$

and

$$\chi_{55} = -k[ML_5^+]/[L]$$

The off diagonal elements of χ are simply the rates of exchange of species between the two sites represented by the particular row and column of the matrix. At sufficiently slow rates of exchange, the exchange contribution to the line width ("$1/T_2$") for the ith site is given by χ_{ii}. Under these conditions, the line widths for the RhL_5^+ resonances should be independent of both $[ML_5^+]$ and $[ML_4^+]$ (eq 16 and 18). However, if [L] and/or $[ML_4^+]$ are sufficiently small, eq 16, 19, and 20 indicate that the preexchange lifetimes at these sites of low population may be very short; at the same time, the preexchange lifetime at the other sites may be long enough for the resonances associated with them to appear to be at or near the "slow exchange limit". Figure 2 shows the dependence of the line widths for both ML_5^+ sites as a function of [L]/[M] ([M] = $[ML_5^+]$ + $[ML_4^+]$) under these conditions. The parameters used in this calculation were $[ML_5^+]$ + $[ML_4^+]$ = 0.125 mol l.$^{-1}$, K = $[ML_4^+][L]/[ML_5^+]$ = 10^{-5} mol l.$^{-1}$, and k_1 = 100 s^{-1}. The site frequencies were ν_1, ν_2 = 320 Hz, 138 Hz (ML_5^+), ν_3, ν_4 = 417 Hz, 213 Hz (ML_4^+), ν_5 = 0 Hz (L). These values are typical for the system with M = Rh, L = $P(OCH_3)_3$ near room temperature. The quantity "$1/T_2$" plotted in Figure 2 is minus the real part of the spectral vector[8] associated mainly with the ML_5^+ sites. The contributions of relaxation to the line widths have not been included since they are in practice negligible at exchange rates (k_1) near 100 s^{-1}. "$1/T_2$" is a measure of the exchange contributions to line widths at the two ML_5^+ sites. The results shown in Figure 2 cover the range [L]/[M] = 4 (pure ML_4^+) to [L]/[M] = 6.0 (equimolar ML_5^+ and L).

It can be seen that the previous predictions of a factor of nine increase in line width on adding ML_4^+ to ML_5^+ and of a factor of two on adding L to ML_5^+ obtained from the four- and three-site approximations in our earlier work[4] are accurately reproduced. The relative line widths for the $ML_5^+ + ML_4^+$, ML_5^+, $ML_5^+ + L$ systems are in the same proportion as the reciprocals of the "effective" preexchange lifetimes $(10/9k_1)^{-1}:(10/k_1)^{-1}:(5/k_1)^{-1}$.

Experimental confirmation of the expected behavior of the ML_5^+ line widths, at constant temperature as [L]/[M] is varied, is given in Figure 3 where the observed and calculated line widths for line 1 (ν = 138 Hz, Figure 1) are shown over the concentration range [L]/[M] = 4 to [L]/[M] = 6 [L = $P(OCH_3)_3$] at 18 °C. It can be seen that the observed and calculated line widths are in quite good quantitative agreement throughout the whole range of [L]:[M] ratios. The observed behavior in Figure 3 is *inconsistent* with a predominantly associative mechanism.

The preexchange lifetimes for ML_4^+ and free L can be obtained from eq 19 and 20. For the conditions used to obtain Figure 2, we find $\tau_L \leqslant \sim 10^{-4}$ s for [L]/[M] $\leqslant$ 5 and $\tau_{ML_4^+} \leqslant \sim 10^{-4}$ s for [L]/[M] $\geqslant$ 5 indicating that the L sites have associated fast "exchange limit rates" for [L]/[M] $\leqslant$ 5 and the ML_4^+ sites have associated "fast exchange limit" rates for [L]/[M] $\geqslant$ 5 while the ML_5^+ sites have associated exchange rates typical of a near "slow exchange limit" situation. For [L]/[M] $\sim$ 5 both τ_L and $\tau_{ML_4^+}$ are very short.

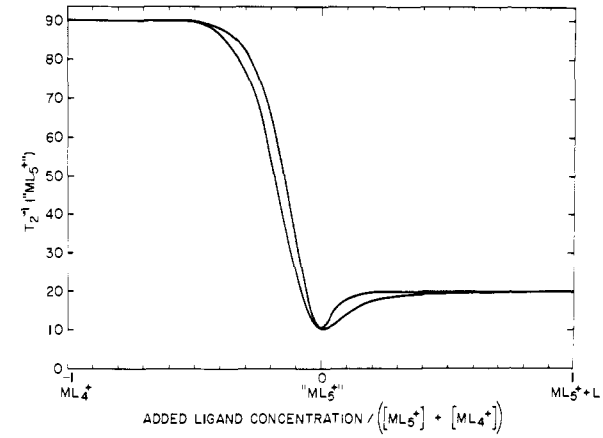

Figure 2. Calculated half widths, $T_2^{-1}(ML_5^+)$, of the components of the $^{31}P\{^1H\}$ doublet (M has nuclear spin I = ½) as a function of total L concentration. The parameters used are: [M] = 0.125 M, K = 10^{-5} M, k_1 = 100 s^{-1}. The two curves correspond to the slightly differing behavior of the two components of the doublet. Only the exchange contributions to the line widths are shown.

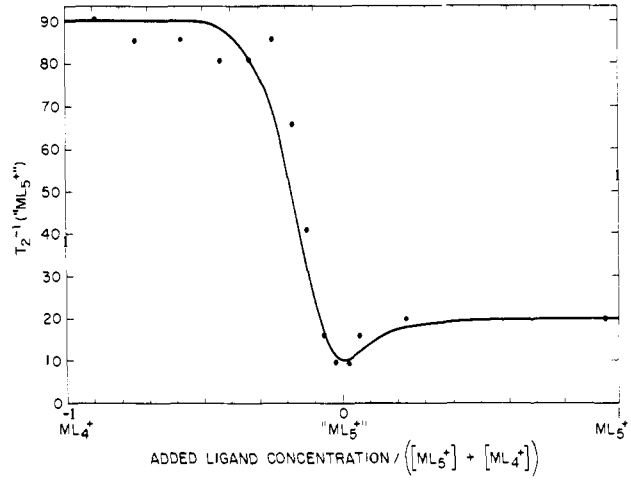

Figure 3. Observed and calculated plots of the exchange contribution to T_2^{-1} for the $^{31}P\{^1H\}$ doublet of $Rh[P(OCH_3)_3]_5^+$ as a function of total L concentration in CH_3CN at 27 °C.

$$k_1\frac{[ML_5^+]}{[ML_4^+]}\mathbf{E} \gg i(\mathcal{L}_3{}^{\omega})_{od} \text{ and } k_1\frac{[ML_5^+]}{[ML_4^+]}\mathbf{E} \gg i(\mathcal{L}_4{}^{\omega})_{od}$$

are well satisfied.[13]

(c) The Three-Site Model for Cases Where the Central Metal Has Zero Spin. If the central metal has no nuclear spin, the five-site model discussed above simplifies to a three-site model with the three sites ML_5^+, ML_4^+, and L. The line shape expression analogous to eq 16 is eq. 21:

$$I(\omega) = -Re\left\{[5[ML_5^+], 4[ML_4^+], L]\begin{bmatrix} -k - 1/T_2 + i(\omega_1 - \omega) & 4k_1/5 & k_1/5 \\ k_1[ML_6^+]/[ML_4^+] & -k_1[ML_5^+]/[ML_4^+] & 0 \\ & -1/T_2 + i(\omega_2 - \omega) & \\ k_1[ML_5^+]/[L] & 0 & -k_1[ML_5^+]/[L] - 1/T_2 + i(\omega_3 - \omega) \end{bmatrix}^{-1}\begin{bmatrix}1\\1\\1\end{bmatrix}\right\} \qquad (21)$$

A plot of "ML_5^+" line width against [L]/[M] is shown in Figure 4 for four different dissociation constants K = 10^{-5} M (lower curve), 10^{-4}, 10^{-3}, and 10^{-2} M (upper curve). The site frequencies used in this calculation were ν_1 = 200 Hz (ML_5^+), ν_2 = 350 Hz (ML_4^+), and ν_3 = 0 Hz (L), and k_1 was kept constant at 100 s^{-1}. The plot is similar to that shown in Figure 2. Again, the "ML_5^+" line widths are strongly dependent on the concentration of added L or ML_4^+ despite the dissociative model used in the calculations.

The above considerations indicate that the condition given in eq 5 is fairly well satisfied for [L]/[M] = 5. This condition is satisfied even better in the case of ML_5^+/ML_4^+ mixtures where [L] is much lower than in "pure" ML_5^+. Similarly, for [L]/[M] $\geqslant$ 5, the corresponding conditions

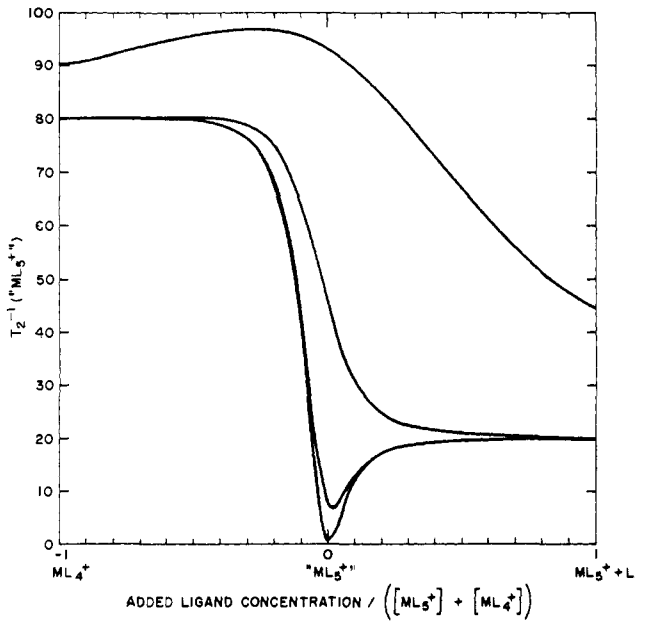

Figure 4. Calculated half width of the $^{31}P\{^1H\}$ resonance for an ML_5^{n+} complex (M has no nuclear spin) as a function of total L concentration. Again, only the contributions of intermolecular exchange are shown. The dissociation constants are (from bottom to top) 10^{-5}, 10^{-4}, 10^{-3}, and 10^{-2} M. The total metal concentration ([M] = $[ML_4^+]$ + $[ML_5^+]$) was set at 0.125 M.

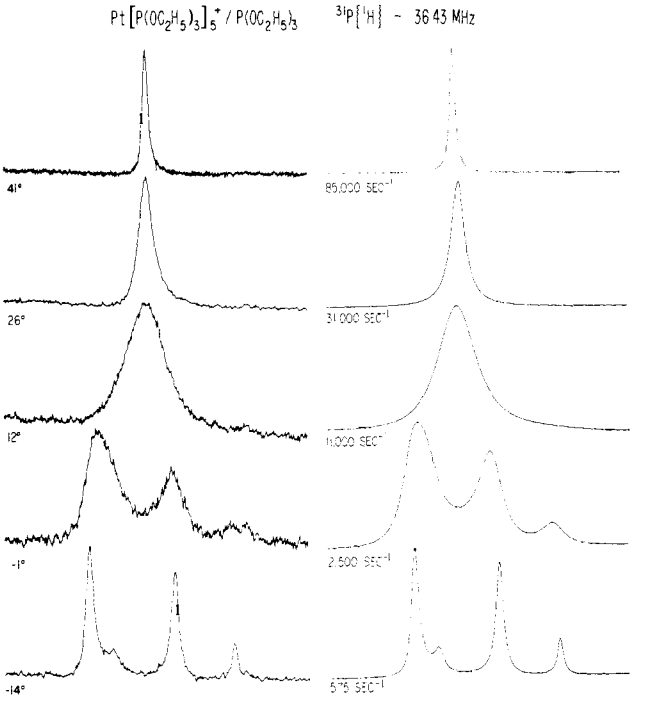

Figure 5. Observed and calculated $^{31}P\{^1H\}$ 36.64-MHz spectra for $Pt[P(OC_2H_5)_3]_5^{2+}$ + $P(OC_2H_5)_3$ in acetonitrile over the temperature range where intermolecular exchange effects can be observed. The spectral width is 9090 Hz.

Results

(a) Spectrophotometric Data. We have assumed in ref 4, and in the earlier part of this paper, that the degrees of ligand dissociation for the ML_5 complexes studied are in general small. Spectrophotometric experiments were performed to measure the equilibrium constants for the species $Rh[P(OCH_3)_3]_5^+B(C_6H_5)_4^-$ and $Rh[P(O\text{-}n\text{-}C_4H_9)_3]_5^+B(C_6H_5)_4^-$. These represent the two extremes of steric size in the series of *n*-alkyl phosphite complexes investigated.

An acetonitrile solution of $Rh[P(OCH_3)_3]_5^+$ + $Rh[P(OCH_3)_3]_4^+$, 0.125 M in rhodium, was determined to be 78% RhL_4^+ and 22% RhL_5^+ by $^{31}P\{^1H\}$ NMR. Room temperature spectrophotometric studies were carried out on a 2.6×10^{-4} M solution of the same sample, and the solution was shown to obey Beer's law. Portions (2 μl) of a 0.025 M solution of $P(OCH_3)_3$ were added to 3 ml of solution and the spectra were recorded in the region 500–300 nm. The absorption band monitored (385 nm) corresponded to RhL_4^+. Qualitative examination of the spectra indicated that, even at 2.6×10^{-4} M, essentially all of the ligand is associated. Using this assumption, $K_{298} = 1 \times 10^{-5}$ mol l.$^{-1}$ and $\Delta G_{298} = -RT \ln K = 6.8$ kcal mol^{-1}.

An acetonitrile solution of $Rh[P(O\text{-}n\text{-}C_4H_9)_3]_5^+$ + $Rh[P(O\text{-}n\text{-}C_4H_9)_3]_4^+$ was determined to be ~100% RhL_4^+ by ^{31}P NMR. Room temperature spectrophotometric studies were carried out on a 3.9×10^{-4} M solution of the same sample. In both cases about 15 points were recorded. The equilibrium constant was determined to be $K_{298} = 3.5 \times 10^{-4}$ mol l.$^{-1}$ and $\Delta G_{298} = 4.7$ kcal mol^{-1}.

The data provide quantitative support for our previous assumption that the complexes have small degrees of dissociation, and the assumption that complexes with ligands of larger steric bulk will have larger degrees of dissociation (a factor of about 30 from $P(OCH_3)_3$ to $P(O\text{-}n\text{-}C_4H_9)_3$).[14]

(b) Intermolecular Exchange for $M[P(OC_2H_5)_3]_5^{n+}$ Complexes (M = Co, Rh, Ir, Ni, Pd, Pt). The data for intermolecular exchange are much more difficult to obtain than were the corresponding data for intramolecular exchange (ref 4) due to the higher temperatures required for the measurements. This results in complications from decomposition of the complexes. A preliminary study suggested that the triethyl phosphite complexes afforded the best chance of obtaining data for all six metals. Slow exchange limit NMR parameters for these and other ML_5 complexes are given in ref 4; this reference also contains synthetic details applicable to all complexes discussed in this paper. Figure 5 shows the observed and calculated $^{31}P\{^1H\}$ spectra for $Pt[P(OC_2H_5)_3]_5^{2+}$, in acetonitrile, as a function of temperature (rate) in the range −14 to 41 °C. The spectra were analyzed using a four-site[15] single spin model (site 1 is the ^{31}P resonance of PtL_5^{2+} with Pt of spin zero, sites 2 and 3 corresponding to $^{195}PtL_5^{2+}$, and site 4 to free ligand) for the equilibrium shown in eq 22.

$$Pt[P(OC_2H_5)_3]_5^{2+} \rightleftharpoons Pt[P(oc_2H_5)_3]_4^{2+} + P(OC_2H_5)_3 \quad (22)$$

Since the intramolecular exchange process has not quite reached the fast exchange limit at −14 °C,[4] the effects of mutual exchange were incorporated, at the lower temperatures in the range studied, by using different T_2 values at the three different PtL_5^{2+} sites. At higher temperatures, T_2 was set to the same (large) value at each site. The site frequencies used in the calculations were $\nu_1 = 5050$ Hz, $\nu_2 = 3250$ Hz, $\nu_3 = 6850$ Hz, and $\nu_4 = 2500$ Hz, and $[L]/[ML_5^{2+}]$ was set at 3.5.

The free energy of activation for *intermolecular* exchange, $\Delta G^{\ddagger}$ (inter), at 299 K is given in Table I together with similar data for the corresponding complexes of Co, Rh, Ir, Ni, and Pd. Free energies of activation for *intramolecular* exchange, $\Delta G^{\ddagger}$ (intra), taken from ref 5 are included in the table for the case where the ligand is $P(OCH_2)_3CCH_3$. The data for *intramolecular* exchange for the $M[P(OCH_2)_3CCH_3]_5$ compounds are accurate to ±0.2 kcal mol^{-1}. Complexes with this ligand were used for comparison since it is the only ligand for which the intramolecular exchange data are available for all six metals. Comparison with the other data in ref 5 suggests

Table I. Free Energies of Activation for Ligand Dissociation and Intramolecular Rearrangement in ML_5 Complexes

Compound	$\Delta G^{\ddagger}$ (inter), kcal mol^{-1} (L = $P(OEt)_3$)	T, K	$\Delta G^{\ddagger}$ (intra), kcal mol^{-1} (L = $P(OEt)_3$)	T, K	$\Delta G^{\ddagger}$ (intra), kcal mol^{-1} (L = $P(OCH_2)_3CCH_3$)	T, K	$\Delta\Delta G^{\ddagger}$, kcal mol^{-1} (L = $P(OEt)_3$)
CoL_5^+	17.9[b]	390	12[a]		10	200	6
IrL_5^+	>14.5[b]	410	10.4	215	8.4	200	>4
NiL_5^{2+}	14.5[b]	350	10.3[a]		8.3	200	4
RhL_5^+	13.8[c]	333	9.9	208	7.8	153	3.9
PtL_5^{2+}	10.5[c]	300	9.2	199	7.0	147	1.3
PdL_5^{2+}	8.5[c]	200	8.0	200	5.7	127	0.5

[a] Not measured directly; estimated from corresponding $P(OCH_2)_3CCH_3$ complex. [b] Benzonitrile solution. [c] Acetonitrile solution.

Table II. Free Energies of Activation for Ligand Dissociation and Intramolecular Exchange in RhL_5 Complexes[a]

Compound	$\Delta G^{\ddagger}$ (inter), kcal mol^{-1}	T, K	$\Delta G^{\ddagger}$ (intra), kcal mol^{-1}	T, K	$\Delta\Delta G^{\ddagger}$, kcal mol^{-1}
$Rh[P(OCH_3)_3]_5^+$	14.0	333	7.5	200	6.5
$Rh[P(OC_2H_5)_3]_5^+$	13.8	333	9.9	208	3.9
$Rh[P(O\text{-}n\text{-}C_3H_7)_3]_5^+$	13.9	333	10.7[b]		3.2
$Rh[P(O\text{-}n\text{-}C_4H_9)_3]_5^+$	14.3	333	11.1	228	3.2
$Rh[P(OCH_2)_3CCH_3]_5^+$	16.8	333	7.5	210	9.3

[a] Solutions in acetonitrile. [b] Estimated from the other *n*-alkyl values.

that the same trend in barriers to intramolecular exchange occurs for $P(OC_2H_5)_3$, with the barriers ~2 kcal mol^{-1} higher (measured and estimated values of $\Delta G^{\ddagger}$ (intra) for the $P(OC_2H_5)_3$ complexes are also included in Table I). A comparison of the barrier trends for the intra- and intermolecular cases shows that the ordering relationship established for intramolecular exchange in ref 5 (Co > Ir ~ Ni > Rh > Pt > Pd) appears to be followed for intermolecular exchange.

(c) Intermolecular Exchange for RhL_5^+ Complexes [L = $P(OCH_3)_3$, $P(OC_2H_5)_3$, $P(O\text{-}n\text{-}C_3H_7)_3$, $P(O\text{-}n\text{-}C_4H_9)_3$, $P(OCH_2)_3CCH_3$]. Figure 6 shows a typical series of temperature dependent $^{31}P\{^1H\}$ NMR spectra for complexes in this category. The spectra are for a solution containing 0.1 M $Rh[P(OC_2H_5)_3]_5^+B(C_6H_5)_4^-$ and 0.625 M $P(OC_2H_5)_3$ in acetonitrile.

The free energy data for intermolecular exchange, $\Delta G^{\ddagger}$ (inter), for the series of complexes are given in Table II together with the corresponding data for intramolecular exchange, $\Delta G^{\ddagger}$ (intra), taken from ref 5. For the *n*-alkyl phosphites, $\Delta G^{\ddagger}$ (inter) is essentially invariant to increasing length of the side chain within the experimental error. This is to be contrasted with the well-established large increases in $\Delta G^{\ddagger}$ (intra) for the same series of compounds.[5]

(d) Solvent Effects. The data presented in he previous sections clearly show that we are dealing with a first-order ligand dissociation process. It is of interest to know whether the solvent plays a significant role in the reaction. To this end, the rate of ligand dissociation has been measured for the reaction

$$Rh[P(OCH_3)_3]_5^+ \rightleftharpoons Rh[P(OCH_3)_3]_4^+ + P(OCH_3)_3 \quad (23)$$

in the seven solvents shown below at 65 °C. The solvents cover quite a wide range of chemical character and dielectric constant. The measured rate of dissociation at 65 °C is the same, within the experimental error, for all seven solvents indicating that there is no significant solvent participation in the forward reaction. The solvents could significantly alter the equilibrium constant by coordination to RhL_4^+ so that the rate of the reverse reaction could have an appreciable solvent dependence.

Solvent	Dielectric constant (25 °C)	Solvent	Dielectric constant (25 °C)
CH_3CN	35	Tetrahydrofuran	8
C_6H_5CN	25	C_6H_5Cl	6
$(CH_3)_2CO$	21	$C_6H_5CH_3$	2.5
Pyridine	12		

Discussion

There have been many studies of substitution reactions in planar d^8 transition metal complexes.[16-18] However, information about the nature of the transition states and the role of possible intramolecular processes has been difficult to obtain. It is clear that the reactions studied in this paper

$$ML_4 + L \underset{k_1}{\overset{k_{-1}}{\rightleftharpoons}} ML_5 \quad (24)$$

may be viewed as planar substitution reactions.[19] Planar four coordinate and trigonal bipyramidal five coordinate forms can be isolated for the same metal-ligand combination, allowing the starting material (ML_4) and what is usually assumed to be the reactive intermediate or transition state for planar substitution (ML_5) to be studied spectroscopically; all ligands are the same leading to maximum skeletal symmetry in reactants, products, and along the reaction coordinate. Thus, the nuclear resonance studies have been used to establish stereochemistry, study intramolecular rearrangements, and measure kinetic and thermodynamic parameters for ligand association-dissociation processes at equilibrium with identical entering and leaving groups.

The $\Delta G^{\ddagger}$ (inter) data are all consistent with process (eq 24) with k_1 independent of solvent or added ligand concentration. The data in Table I show the same ordering for constant ligand as was previously established for $\Delta G^{\ddagger}$ (intra),[5] $Co^+ > Ir^+ \approx Ni^{2+} > Rh^+ > Pt^{2+} > Pd^{2+}$, giving the following inequalities between adjacent members in the periodic table

$$\begin{array}{ccc} Co & > & Ni \\ \vee & & \vee \\ Rh & > & Pd \\ \wedge & & \wedge \\ Ir & > & Pt \end{array}$$

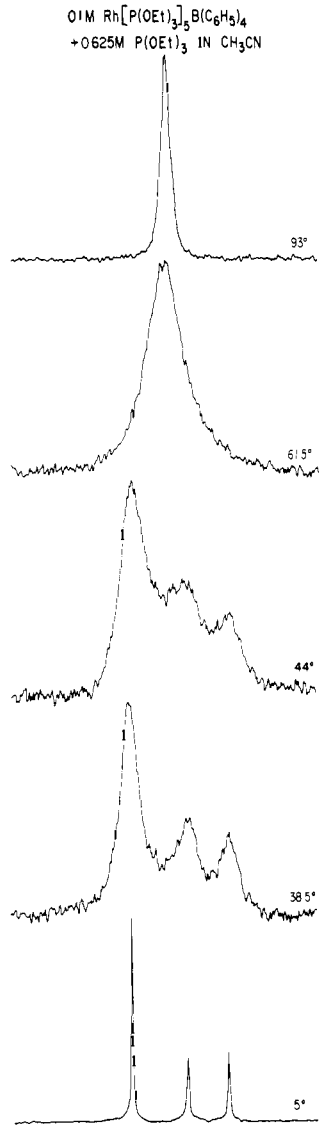

Figure 6. $^{31}P\{^1H\}$ NMR for a solution containing 0.1 M $Rh[P(OC_2H_5)_3]_5^+B(C_6H_5)_4^-$ + 0.625 M $P(OC_2H_5)_3$ in acetonitrile over the temperature range 5–93 °C.

The data in Table II show that $\Delta G^{\ddagger}$ (inter) varies very little as the alkyl side chain is lengthened, in contrast with the well established large increase in $\Delta G^{\ddagger}$ (intra).

Figure 7A shows a model for intermolecular ligand exchange involving a planar four coordinate species (SP), a series of tetragonal pyramidal five coordinate stereochemistries along the reaction coordinate (TP···TP′), and a trigonal bipyramidal five coordinate species (TBP). The entering group attacks perpendicular to the plane of the four coordinate complex ending in the equatorial plane of the five coordinate compound along with two trans ligands of the planar molecule.[21] For an ML_4^{n+} compound, there is an equal probability of either equivalent pair of trans ligands ending in the equatorial plane; for four coordinate complexes with inequivalent ligands, the TP transition state (or intermediate) does not have C_{4v} symmetry and the stereochemical course of the reaction will be towards the energetically preferred TBP species {e.g., in $HM[P(C_2H_5)_3]_3^+$ complexes the trans $P(C_2H_5)_3$ groups go exclusively to the TBP "equatorial" plane and the hydride ligand and the $P(C_2H_5)_3$ ligand trans to it goes to axial positions}.[22,23] Intramolecular exchange in the five coordinate species (Figure 7B) involves trigonal bipyramidal ground states and tetragonal pyramidal transition states.

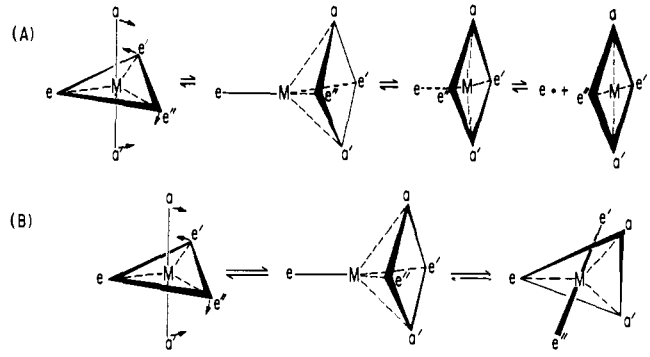

Figure 7. Reaction path for ligand dissociation (A) and for intramolecular rearrangement (B). The labeling of the various stereochemistries is the same in Figures 8 and 9: TBP = trigonal bipyramid, TP = tetragonal pyramid, TP′ = tetragonal pyramid with elongated axial bond, SP = square plane, L = free ligand.

The evidence for these models may be summarized as follows:

(i) The ML_5 Ground State. $^{31}P\{^1H\}$ NMR evidence for trigonal bipyamidal ground states in over 20 ML_5 complexes has been presented previously.[5]

(ii) **The Reaction Coordinate for Intramolecular Rearrangement.** Rearrangement has been shown to involve simultaneous exchange of two axial with two equatorial ligands.[5] The tetragonal pyramid is the simplest intermediate for effecting this change[24] and many of the geometries required by the reaction coordinate have been found in crystal structure studies.[25] Barriers are commonly less than 4 kcal mol^{-1}, comparable to crystal packing forces. Deformations will occur most easily in the direction requiring the smallest free energy change in the isolated molecule, i.e., along the reaction coordinate for intramolecular rearrangement.

(iii) **The ML_4 Ground State.** Crystallographic evidence for planar or near-planar geometries in four coordinate Pt^{2+}, Pd^{2+}, Ir^+, and Rh^+ chemistry is abundant. It is probable that most of the ML_4^{n+} complexes considered here are planar, possibly with distortions in some cases due to steric crowding. However, there is the very real possibility in some cases of solvent coordination leading to ML_4S^{n+} five coordinate complexes. These would be fluxional and could also account for the diamagnetic, single line character of NiL_4^{2+} and CoL_4^+ solutions.[19]

(iv) **The Reaction Coordinate for Ligand Association.** The evidence for attack of L along the pseudo-C_4 axis of planar HML_3^+ cations, leaving the ligand trans to hydride unique, shows unambiguously that the dissociating group in HML_4^+ complexes comes from an "equatorial" site.[22,23] Extrapolation of this conclusion to the ML_4–ML_5 case is reasonable. C_4 attack and equatorial dissociation have been incorporated in Figure 7A.[21]

The identical trends in barriers for inter- and intramolecular exchange, as M is varied (Table I), suggest that similar or identical geometries occur along the two reaction coordinates. Tetragonal pyramidal geometries have been incorporated in both reaction coordinates in Figure 7. Schematic free energy changes along the reaction coordinates are shown in Figure 8. If the intermediate (solid line) or transition state (dotted line) for intramolecular exchange (TP) occurs also on the reaction coordinate for ligand association-dissociation (this does not necessarily have to be the case, but appears reasonable in view of the data presented in this paper), then only the bottom part of Figure 8 is necessary. Intramolecular exchange can be effected by population of the TP state followed by return over the lower barrier to a rearranged trigonal bipyramid. $\Delta G^{\ddagger}$ (intra) does not necessarily have to appear as a well-defined maximum in the bottom part of Figure 8. The geometrical

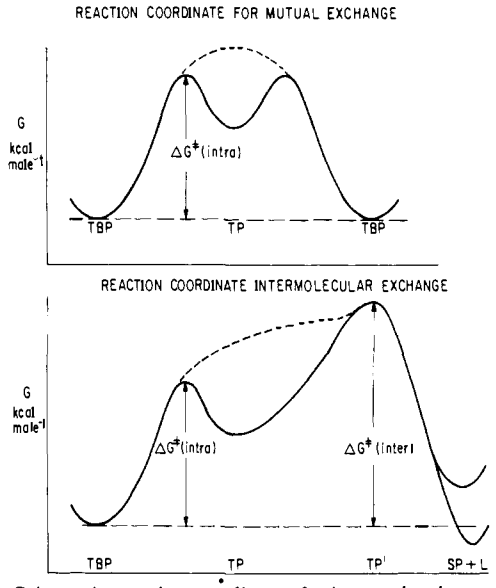

Figure 8. Schematic reaction coordinates for intramolecular rearrangement (top) and ligand association–dissociation (bottom) in ML_5 complexes: TBP = trigonal bipyramid, TP = tetragonal pyramid, TP′ = tetragonal pyramid with elongated axial bond, SP = square plane, L = free ligand. The solid curves correspond to situations in which TP is an intermediate; the dotted curves where it is a transition state. At the SP + L point in the bottom half of the diagram, curves are given for SP less stable than TBP (this covers all cases in the present paper) and for SP more stable than TBP (this is true for cases in which L is sterically bulkier e.g., $Rh[P(OC_6H_5)_3]_4^+$).

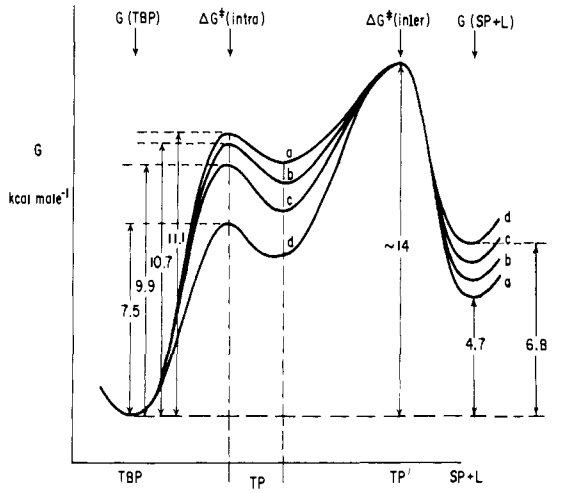

Figure 9. Schematic reaction coordinates for ligand association–dissociation in RhL_5 complexes: TBP = trigonal bipyramid, TP = tetragonal pyramid, TP′ = tetragonal pyramid with elongated axial bond, SP = square plane, L = free ligand. (The curves do not necessarily have to have minima in the middle, particularly if the coordinate for intramolecular exchange alone has no minimum.) A family of curves is shown which semiquantitatively represent the situation for the RhL_5^+ complexes: (a) L = $P(O\text{-}n\text{-}C_4H_9)_3$, (b) L = $P(O\text{-}n\text{-}C_3H_7)_3$, (c) L = $P(OC_2H_5)_3$, (d) L = $P(OCH_3)_3$.

correspondence between Figures 7 and 8 is shown by the symbols TBP, TP, TP′, SP, and L.

With this picture, the following additional refinements are possible. It has been shown in earlier work[5] that the value of $\Delta G^{\ddagger}$ (intra) increases sharply with increasing steric bulk of the ligand for a given metal, due to steric crowding of the tetragonal pyramid relative to the trigonal bipyramid. Table II shows that the corresponding $\Delta G^{\ddagger}$ (inter) values for the rhodium *n*-alkyl phosphite complexes are almost constant. The overall invariance of $\Delta G^{\ddagger}$ (inter) in this series might be expected from electronic considerations. The steric bulk of the four ligands in this series is quite different; however, the electronic properties are quite similar. This would be in accord with an intermolecular process involving bond breaking. The effects along the reaction coordinate may be viewed as an increase in $\Delta G^{\ddagger}$ (intra) due to steric crowding in achieving the TP state with an offsetting steric assist to ligand dissociation in TP. $\Delta G^{\ddagger}$ (inter) − $\Delta G^{\ddagger}$ (intra) = $\Delta\Delta G^{\ddagger}$ being a rough measure of the additional free energy required to break the axial bond in TP (particularly if *TP* is a *transition state* for intramolecular rearrangement). A family of semiquantitative free energy curves for the RhL_5^+ complexes (L = *n*-alkyl phosphite) is shown in Figure 9. The curves have been normalized to coincide at the TBP point. The tetragonal pyramidal geometry occurs near one vertical dotted line in the figure—to the left if there is no minimum in the reaction coordinate for intramolecular exchange, to the right if there is; intramolecular exchange can be effected by population of the tetragonal pyramidal state followed by return to a rearranged trigonal bipyramid. The geometrical correspondence between Figures 7 and 9 is again shown by the symbols TBP, TP, TP′, SP, and L.

The SP + L point, unlike the rest of the curve, is likely to be quite sensitive to solvent; we have shown with the spectrophotometric studies that the equilibrium constants for dissociation (a function of $G(P + L) - G(TBP)$), will increase as the steric bulk of L increases, making curve a the lowest at the (SP + L) position. The actual free energy differences between TBP and SP + L for the $P(OCH_3)_3$ (curve d) and $P(O\text{-}n\text{-}C_4H_9)_3$ (curve a) complexes in CH_3CN have been used in constructing the right side of Figure 9.

The $\Delta\Delta G^{\ddagger}$ data in Table II suggest that a significantly higher energy is required to break the bond in TP for $P(OCH_2)_3CCH_3$ vs. $P(OCH_3)_3$, even though the $\Delta G^{\ddagger}$ (intra) values indicate similar steric sizes. The difference presumably arises from a significantly larger electronic contribution to the Rh–P bond strength in the $P(OCH_2)_3CCH_3$ complex relative to the *n*-alkyl phosphites. This is consistent with the spectrophotometric evidence for a higher ligand field in CoL_5^+ and NiL_5^{2+} complexes with this ligand compared to acyclic $P(OCH_3)_3$ which has previously been reported by Verkade and co-workers.[26]

It is, of course, not necessary that a species identical with the transition state in Figure 7B occur in the reaction coordinate Figure 7A; however, on the basis of the results discussed above, passage through a tetragonal pyramidal form (possibly with different bond angles and bond lengths to those in intramolecular process) in the association reaction seems a much more plausible mechanism than a process in which *a*, *M*, and *a′* always remain collinear (their initial and final relationship in Figure 7A). This latter scheme is the one commonly drawn when representing planar association reactions.

Conclusions

The unusual line width effects found in the $Rh[P(OCH_3)_3]_5^+/Rh[P(OCH_3)_3]_4^+/P(OCH_3)_3$ system[4] have been confirmed using a complete five-site calculation assuming a first-order dissociative mechanism, and the interpretation has been further supported by additional line width studies at constant temperature. Qualitatively, the effects arise because pseudo-first-order rate constants for some of the processes can lie near to "slow exchange" rates while, at the same time, others are fast.

Overall, the following features of planar substitution reactions have been demonstrated: (1) Presence of a trigonal bipyramidal intermediate (in this case, product). (2) Strict first-order dissociative process for the reverse reaction, with a rate independent of solvent. (3) Observation of ligand association and intramolecular rearrangement (pseudorotation)

in the same system. (4) Direct observation of a steric influence on the equilibrium constant for dissociation.

The following features are suggested: (1) Evidence for tetragonal pyramidal stereochemistries in both the dissociation and pseudorotation reaction coordinates: A strong correlation between the free energies of activation for the two processes, with the differences between the two free energy terms giving a qualitative measure of the additional energy required for bond breaking in the *transition state* for intramolecular rearrangement.

(2) Establishment of two approximately separable steric contributions to the association process, having opposite sign. One, the sterically unfavorable effects of crowding of the basal ligands in the TP intermediate and the other the steric assist to axial bond breaking in TP′. The two effects almost exactly cancel, and may be a reflection of the very similar electronic properties of the ligands involved.

Acknowledgments. We would like to thank Mr. M. A. Cushing for preparation of many of the complexes and Mr. G. Watunya and Mr. F. N. Schoch for obtaining many of the ^{31}P spectra.

References and Notes

(1) J. P. Jesson and P. Meakin, *J. Am. Chem. Soc.*, **95**, 1344 (1973).
(2) J. P. Jesson and P. Meakin, *Inorg. Nucl. Chem. Lett.*, **9**, 1221 (1973).
(3) P. Meakin and J. P. Jesson, *J. Am. Chem. Soc.*, **95**, 7272 (1973).
(4) P. Meakin and J. P. Jesson, *J. Am. Chem. Soc.*, **96**, 5751 (1974).
(5) J. P. Jesson and P. Meakin, *J. Am. Chem. Soc.*, **96**, 5760 (1974).
(6) If the ratio of the populations is large enough, the sites with large populations may still be in their "slow exchange limit" even though the preexchange lifetimes for the sites of low population are very short.
(7) R. G. Gordon and R. P. McGinnis, *J. Chem. Phys.*, **49**, 2455 (1968).
(8) G. Binsch, *J. Am. Chem. Soc.*, **91**, 1304 (1969).
(9) R. E. Shirmer, J. H. Noggle, and D. F. Gaines, *J. Am. Chem. Soc.*, **91**, 6240 (1969).
(10) C. A. Tolman, P. Meakin, D. L. Lindner, and J. P. Jesson, *J. Am. Chem. Soc.*, **96**, 2762 (1974).
(11) The five sites are: (1) RhL_5^+ ^{103}Rh spin up, (2) RhL_5^+ ^{103}Rh spin down, (3) RhL_4^+ ^{103}Rh spin up, (4) RhL_4^+ ^{103}Rh spin down, (5) free ligand.
(12) The spin "density matrices" used in these equations are weighted by their site populations. If unweighted spin "density matrices" ($Tr(\rho_i) = 1$ for each site i) are used, eq 1 can be written as

$$\frac{d\rho_1}{dt} = -i\mathcal{L}_1\rho_1 - k_1\rho_1 + \frac{4k_1}{5}\rho_3 + \frac{k_1}{5}\rho_5 \text{ etc.} \qquad (25A)$$

$$\frac{d\rho_5}{dt} = -i\mathcal{L}_5\rho_5 - \frac{k_1}{5}\frac{[ML_5^+]}{[L]}\rho_5 + \frac{k_1}{5}\frac{[ML_5^+]}{2[L]}(\rho_1 + \rho_2) \qquad (25E)$$

Equation 3 must then be replaced by

$$I(\omega) \propto Im(\rho^\omega \cdot \sigma^-) \qquad (26)$$

where σ^- is a vector containing the elements of the spin lowering operators $\mathbf{M}_1^-$ weighted by their site populations. The NMR line shape can, of course, be calculated using either eq 2 and 3 or 25 and 26, and sites of very low concentration can be eliminated from eq 25 and 26 in the same way that they were eliminated from eq 2 and 3.
(13) In general, the inequality $\mathbf{A} \gg \mathbf{B}$ means $(\mathbf{A} + \mathbf{B})^{-1} \rightarrow \mathbf{A}^{-1}$.
(14) A. D. English, P. Meakin, and J. P. Jesson, *Inorg. Chem.* **15**, 1233 (1976).
(15) A more complete treatment in this case would employ a seven-site model. However, under the conditions of this experiment $[PtL_4^{2+}]$ is very small and the three PtL_4^{2+} sites can be eliminated as described above.
(16) D. A. Redfield and J. H. Nelson, *J. Am. Chem. Soc.*, **96**, 6219 (1974) (and earlier references).
(17) J. Powell and D. G. Cooper, *J. Chem. Soc., Chem. Commun.*, 749 (1974), and earlier references.
(18) L. Cattalini, *MTP Int. Rev. Sci., Ser. 1*, **9**, 269 (1972); C. H. Langford and H. B. Gray, "Ligand Substitution Processes", W. A. Benjamin, New York, N.Y., 1966.
(19) We are grateful to E. L. Muetterties for pointing out the existence of stable $ML_4(solvent)^{n+}$ species.[20] He has shown that $Co[P(OCH_3)_3]_4(CH_3CN)^+$ can be isolated and in solution gives rise to $^{31}P\{^1H\}$ NMR spectra which are AB_3 patterns. It is possible, therefore, that our NiL_4^{2+} and CoL_4^+ solutions exhibit diamagnetic behavior because of solvent coordination rather than because of planar geometries. The whole question of the nature of ML_4^{n+} complexes in solution is being investigated in detail and will be reported at a later date. It is possible that equilibria of the form

$$ML_4(S)^{n+} \overset{-S}{\rightleftharpoons} [ML_4^{n+}]_{planar} \rightleftharpoons [ML_4^{n+}]_{tetrahedral}$$

$$[ML_4^{n+}]_{planar} + L \rightleftharpoons ML_5^{n+}$$

will have to be invoked for some metals.
(20) E. L. Muetterties (private communication).
(21) E. L. Muetterties has suggested[20] that the reaction coordinate might not have fourfold symmetry in the early stages of the substitution process, since there will be a repulsion between the ligand lone pair and the metal d_{z^2} electrons. This is certainly possible and will depend on the details of the rehybridization process. Such an effect would be difficult to establish experimentally.
(22) P. Meakin, R. A. Schunn, and J. P. Jesson, *J. Am. Chem. Soc.*, **96**, 277 (1974).
(23) A. D. English, P. Meakin, and J. P. Jesson, *J. Am. Chem. Soc.*, **98**, 422 (1976).
(24) R. S. Berry, *J. Chem. Phys.*, **32**, 933 (1960).
(25) E. L. Muetterties and L. J. Guggenberger, *J. Am. Chem. Soc.*, **96**, 1948 (1974).
(26) J. G. Verkade, *Coord. Chem. Rev.*, **9**, 1 (1972).